

Synthesis and structure of boron-bridged constrained geometry complexes of titanium

Holger Braunschweig,^{*a} Frank M. Breitling,^{a,b} Carsten von Koblinski,^c Andrew J. P. White^{†b} and David J. Williams^b

^a Institut für Anorganische Chemie, Julius-Maximilians-Universität Würzburg, Am Hubland, D-97074 Würzburg, Germany

^b Imperial College London, Exhibition Road, London, UK SW7 2AZ

^c Institut für Anorganische Chemie, RWTH Aachen, Templergraben 55, D-52056 Aachen, Germany

Received 3rd December 2003, Accepted 5th February 2004

First published as an Advance Article on the web 13th February 2004

The boron-bridged constrained geometry titanium complexes $[\text{Ti}\{\eta^5\text{-}\eta^1\text{-}(\text{C}_5\text{H}_4\text{B}(\text{NR}_2)\text{NPh}\})(\text{NMe}_2)_2]$ [$\text{R} = i\text{Pr}$ (**3**), SiMe_3 (**4**)] and $[\text{Ti}\{\eta^5\text{-}\eta^1\text{-}(\text{C}_9\text{H}_6\text{B}(\text{N}i\text{Pr}_2)\text{NPh}\})(\text{NMe}_2)_2]$ (**12**) have been prepared in good yields by amine elimination reaction from $[\text{Ti}(\text{NMe}_2)_4]$. Subsequent deamination–chlorination with excess Me_3SiCl yielded the corresponding dichloro-complexes (**5**, **6**, **13**). Reaction of the analogous ligand precursors $(\text{C}_5\text{H}_5\text{B}(\text{N}i\text{Pr}_2)\text{N}(\text{H})\text{R})$ ($\text{R} = \text{Cy}$, $t\text{Bu}$) with $[\text{Ti}(\text{NMe}_2)_4]$ did not result in the expected bridged compounds, but rather in the half-sandwich complexes $[\text{Ti}\{\eta^5\text{-}\text{C}_5\text{H}_4\text{B}(\text{N}i\text{Pr}_2)\text{N}(\text{H})\text{R}\})(\text{NMe}_2)_3]$ [$\text{R} = \text{Cy}$ (**9**), $t\text{Bu}$ (**10**)]. All compounds were fully characterised by means of multinuclear NMR spectroscopy. Thorough investigation of substituent effects was achieved by comparative X-ray diffraction studies on complexes **3**, **5**, **6** and **12**.

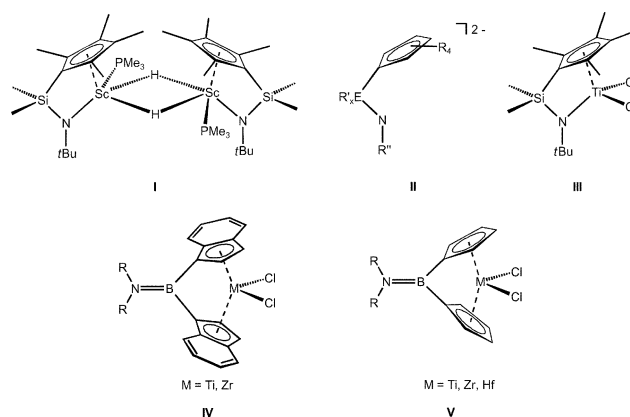
Introduction

Group IV metallocenes have been first studied in polymerisation research because they can be used to model the active sites in the classically heterogeneous Ziegler–Natta type polymerisation of olefins in a homogeneous environment. With the discovery of methylaluminoxane (MAO) as a highly efficient activator, the interest in Group IV metallocenes was shifted from mechanistic studies towards utilisation of these compounds as catalysts on an industrial scale. Due to uncertainties about the structure of MAO, and consequently its interaction with the metallocenes, a clear understanding of the polymerisation process remained elusive.¹ In 1990, Bercaw presented the well-defined scandium complex **I** that is isoelectronic with the proposed cationic active species in Group IV mediated polymerisations of olefins and is itself an active polymerisation catalyst even in the absence of a co-catalyst.²

In due course, groups both in industry and academia employed the same general ligand framework (**II**) to synthesise corresponding Group IV constrained geometry complexes (CGC) such as **III**. Complexation was usually achieved by reaction of the ligand precursor with a suitable metal compound *via* a dilithiation–salt elimination sequence or amine/alkane elimination. CGC of Group IV metals are known to be active olefin polymerisation catalysts when activated with MAO or other co-catalysts.³

The industrial interest in these new systems can be generally attributed to the unique properties of the polymers obtained. The combination of a decreased tendency to undergo β -hydride elimination and an ability to readily incorporate higher α -olefins results in linear polymers with long sidechains. The linear low density polyethylene (LLDPE) produced combines the high processability of low density polyethylene (LDPE), obtained from the ICI radical process, with the strength and toughness of metallocene produced high density polyethylene (HDPE).^{3a,d}

Beside efforts to tune polymerisation characteristics by modification of the cyclopentadienyl (Cp) and amido fragments of the ligand framework, a variety of different bridging moieties were reported.^{3b,c} The bridging moiety affects the



Cp(centroid)–M–N angle and is hence, a crucial parameter in the polymerisation reaction. Extending our synthetic method for the preparation of boron-bridged ligand precursors⁵ and corresponding metallocenes^{6,7} that are stabilised by an amino substituent such as **IV** and **V**, we recently communicated the first boron-bridged CGC of titanium.^{8,9} The very short and rigid bridging moiety in these compounds and its potentially electron withdrawing effect may result in advantageous catalytic properties.¹⁰

In the present paper we report the synthesis of a series of novel boron-bridged CGC of titanium and comparative structural studies of these compounds by means of X-ray analysis.

Results and discussion

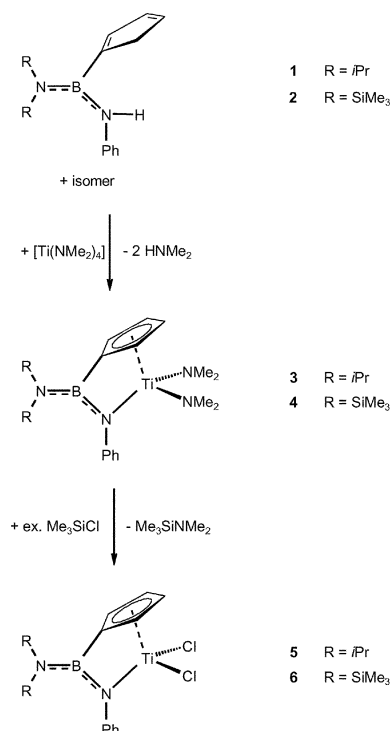
Synthesis and characterisation of new boron-bridged cyclopentadienyl CGC

We have previously reported the synthesis of boron-bridged CGC type ligands.^{5b–d} The incorporating zirconocene, $[\text{Zr}\{\eta^5\text{-}\eta^1\text{-}(\text{C}_9\text{H}_6\text{B}(\text{N}i\text{Pr}_2)\text{NPh}\}_2]$, has been prepared *via* a dilithiation–salt elimination sequence which demonstrated the stability of the boron bridge against nucleophilic attack by lithium alkyl reagents.^{5b} Nevertheless, dilithiation of the ligand precursors $(\text{C}_5\text{H}_5\text{B}(\text{N}i\text{Pr}_2)\text{N}(\text{H})\text{Ph})$ (**1**) and $(\text{C}_9\text{H}_7\text{B}(\text{N}i\text{Pr}_2)\text{N}(\text{H})\text{Ph})$ (**11**) with 2 equiv. of *Li*nBu, reaction with $[\text{TiCl}_3(\text{thf})_3]$ and subsequent oxidation by 0.5 equiv. of PbCl_2

[†] X-Ray crystallography.

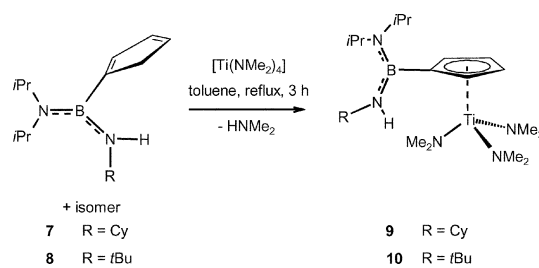
always resulted in product mixtures that could not be separated.¹¹

An amine elimination route, employing $[\text{Ti}(\text{NMe}_2)_4]$, proved to be more fruitful. The reaction of ligand precursors $(\text{C}_5\text{H}_5)\text{-B}(\text{N}i\text{Pr}_2)\text{N}(\text{H})\text{Ph}$ (**1**) and $(\text{C}_5\text{H}_5)\text{B}\{\text{N}(\text{SiMe}_3)_2\}\text{N}(\text{H})\text{Ph}$ (**2**) with $[\text{Ti}(\text{NMe}_2)_4]$ resulted in the formation of the boron-bridged CGC **3**⁸ and **4** (Scheme 1). When $[\text{Ti}(\text{NMe}_2)_4]$ was added to a hexane solution of the respective ligand precursor at -78°C , no reaction in terms of colour change from yellow to dark orange and release of HNMe_2 was observed below -10°C . Yields after recrystallisation were good. Subsequent reaction with Me_3SiCl gave the corresponding dichloro-complexes **5** and **6** in good yields (Scheme 1). Compounds **3**, **5** and **6** were obtained as orange or red crystals, whereas **4** was obtained as a dark red oil. The compounds proved to be air- and moisture-sensitive, very soluble in CH_2Cl_2 and moderately soluble in toluene and hexane.



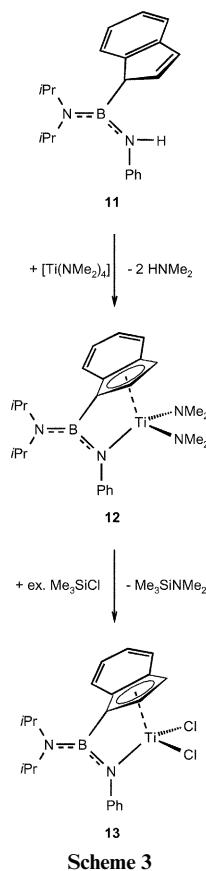
Cp complexes **3–6** were characterised by multinuclear NMR techniques. The ^{11}B NMR chemical shifts of δ 27.8 and 28.4, respectively, for the $i\text{Pr}_2\text{N}$ substituted complexes **3** and **5**, and at δ 33.0 and 33.1, respectively, for the $(\text{Me}_3\text{Si})_2\text{N}$ substituted complexes **4** and **6**, closely resemble those of the respective ligand precursors.^{5d} The relative down field shift for the $(\text{Me}_3\text{Si})_2\text{N}$ substituted compounds **4** and **6**, with respect to those compounds with the $i\text{Pr}_2\text{N}$ substituent on boron, can be attributed to the deshielding effect of the Me_3Si groups. ^1H and ^{13}C NMR spectra for **3–5** display two signals each for the methine groups of the Cp moiety, indicating approximate C_s symmetry in solution. In contrast, the ^1H and ^{13}C NMR spectra of **6** show four sets of signals for the methine groups and the ^{29}Si NMR spectrum displays two signals indicating C_1 symmetry in solution. Such a geometry would appear to arise from a torsion of the $\text{N}(\text{SiMe}_3)_2$ fragment (*vide infra*) and hindered rotation about the $\text{B}-\text{N}(\text{SiMe}_3)_2$ axis. The signals for the *ipso*-C of the Cp ring could not be detected in the room temperature ^{13}C NMR spectra of **3–6** due to quadrupolar $^{13}\text{C}-^{11}\text{B}$ coupling.¹²

In the case of ligand precursors $(\text{C}_5\text{H}_5)\text{B}(\text{N}i\text{Pr}_2)\text{N}(\text{H})\text{R}$ [$\text{R} = \text{Cy}$ (**7**), $t\text{Bu}$ (**8**)] performing the reaction in toluene under reflux conditions resulted only in the formation of the non-bridged half-sandwich complexes **9** and **10** (Scheme 2). This observation



might be both the result of increased steric bulk of the substituents R compared to a phenyl group and a significantly lower acidity of the alkyl-NH in comparison to the phenyl-NH group. The formulations of **9** and **10** are evident from integration ratios in the ^1H NMR spectra as well as from the IR spectra that display characteristic NH stretching bands at 3441 and 3456 cm^{-1} , respectively, for **9** and **10** (in comparison to 3435 and 3454 cm^{-1} , respectively, for the ligand precursors **7** and **8**¹³).

The same synthetic route as outlined above was extended to the preparation of the indenyl CGC **12** and **13** (Scheme 3). In the first step, elevated temperatures and extended reaction times had to be applied to obtain sufficient conversion. While the Cp complexes **3** and **4** were formed very smoothly, the synthesis of the indenyl derivative **12** suffered from the formation of significant amounts of undesired products of the type $[\text{LTi}(\text{NMe}_2)_3]$, where only the indenyl or the amido moiety of the newly introduced ligand is coordinated to the metal centre. The yield was accordingly modest, though after two subsequent recrystallisation steps the analytical pure target compound **12** could be obtained in the form of orange crystals. Deamination-chlorination of **12** with Me_3SiCl gave the dichloro complex **13** in high yield as a red microcrystalline material. ^{11}B NMR chemical shifts of **12** and **13** at δ 27.7 and 28.0, respectively, again resemble the value observed for the ligand precursor.^{5b} ^1H and ^{13}C NMR spectra of **12** and **13** were unremarkable and showed



all of the expected signals apart from the signal for the *ipso*-C of the indenyl moiety.

X-Ray crystallographic analysis of complexes 3, 5, 6 and 12

The molecular structures of **5**, **6** and **12** as determined by single crystal X-ray analysis are shown in Figs. 1–3, respectively. Complex **5** crystallised with two independent molecules (A and B) in the asymmetric unit each having essentially identical geometries – the rms deviation of the best fit between the two molecules is only 0.058 Å. The gross structures of the previously reported species **3**,⁸ and complexes **5**, **6** and **12** are very similar with each exhibiting a characteristic angling of the B–C(1) bond to the [C₅] ring plane (Table 1). There are, however, a few notable differences between the four structures.

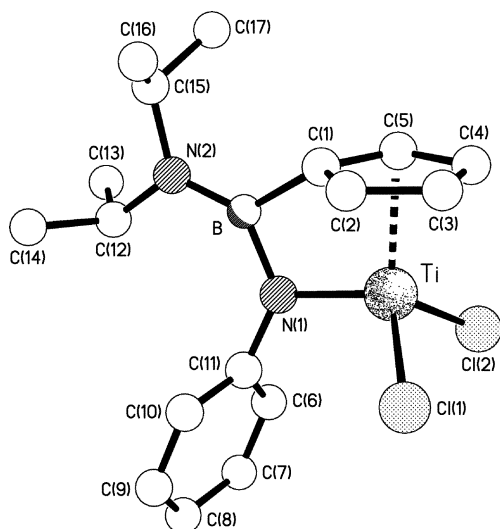


Fig. 1 The structure of one of the two crystallographically independent molecules (A) present in the crystals of **5**. Selected bond lengths (Å) and angles (°) (values for the second independent molecule in square brackets): Ti–Cl(1) 2.260(2) [2.2588(14)], Ti–Cl(2) 2.2677(15) [2.2707(15)]; C₅–Ti–Cl(1) 117.1 [118.5], C₅–Ti–Cl(2) 118.2 [118.6].

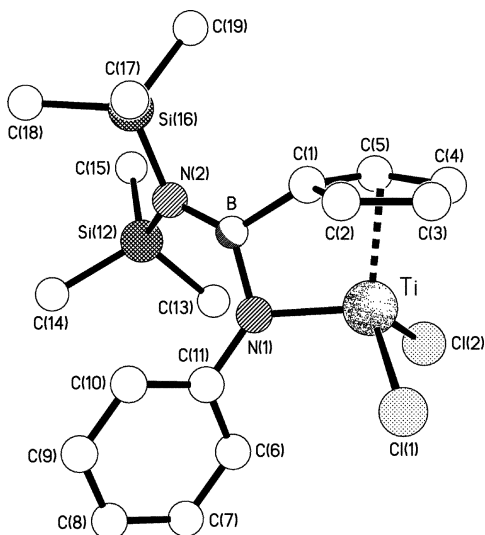


Fig. 2 The molecular structure of **6**. Selected bond lengths (Å) and angles (°): Ti–Cl(1) 2.2385(12), Ti–Cl(2) 2.2553(13); C₅–Ti–Cl(1) 120.3, C₅–Ti–Cl(2) 117.1.

If one considers the C₅ aromatic rings in all four complexes as η¹-moieties, the geometry at titanium can be viewed as distorted tetrahedral with angles in the range 99.2(1)–123.82(11)°, the most acute angle in each case being associated with the bite of the chelating ligand. In each structure the metal centre is slightly displaced (δ) from a position directly underneath the C₅ ring centroid such that the Ti–C₅ ring centroid vector subtends

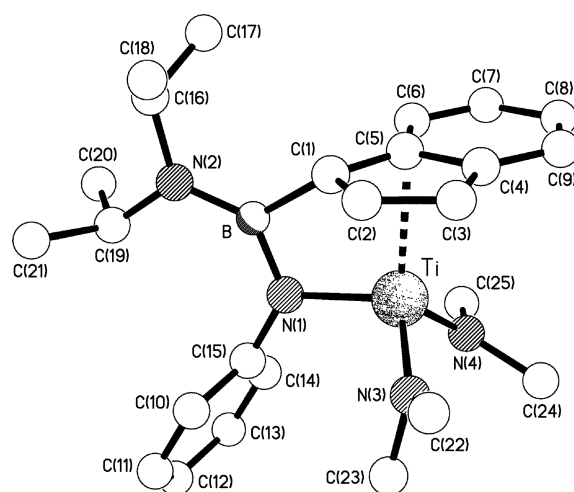


Fig. 3 The molecular structure of **12**. Selected bond lengths (Å) and angles (°): Ti–N(3) 1.915(2), Ti–N(4) 1.918(3); C₅–Ti–N(3) 115.7, C₅–Ti–N(4) 123.8.

an angle (ϕ) of *ca.* 3–5° to the normal to the ring plane. The Ti–C₅ ring centroid and Ti–N(1) bond lengths in **3** and **12** are significantly longer than those observed in **5** and **6** reflecting the very different electronic environments of titanium centres bearing two NMe₂ ligands compared to those with two chlorides. In all four structures both the B and N(2) centres have trigonal planar geometries, but whereas in **3**, **5** and **12** these two trigonal planes are nearly coplanar, in **6** the steric bulk of the SiMe₃ substituents forces a twist of *ca.* 38° between them. This twist, however, is not accompanied by any significant lengthening of the B–N(2) bond, though there is an increased bend of the B–C(1) vector out of the [C₅] ring plane, and a noticeably flatter geometry around N(1).

In the structure of **5** adjacent independent molecules are linked by C–H \cdots π interactions to form an extended chain that propagates along the crystallographic *b* axis (Fig. 4). No significant packing interactions are observed between adjacent molecules in the crystals of **6**, the closest intermolecular contact being the approach of the C(4)–H proton in one molecule to the Cl(1) centre in another [C \cdots Cl 3.74 Å, H \cdots Cl 2.84 Å, C–H \cdots Cl 158°]. There are no noteworthy intermolecular interactions in the crystals of **12**.

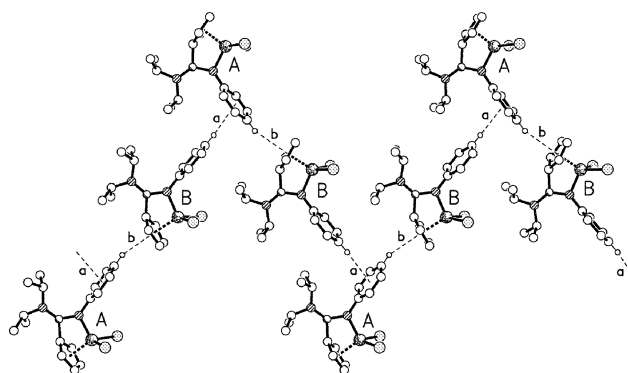


Fig. 4 Part of one of the extended C–H \cdots π linked chains of alternating A and B type molecules present in the crystals of **5**. The hydrogen bonding geometries [H \cdots π] (Å) and [C–H \cdots π] (°) are (a) 2.81, 155 and (b) 2.84, 158.

Conclusions

A series of new boron-bridged constrained geometry complexes of titanium, [Ti{ η^5 : η^1 -(C_xH_y)B(NR₂)NPh}R'₂], has been prepared and some have been structurally characterised. It has been demonstrated that the chelating ligand framework can readily be altered by modification of the η^5 -coordinated frag-

Table 1 Comparative selected geometric parameters for complexes **3**,⁸ **5**, **6** and **12**

	3	5 (mol. A)	5 (mol. B)	6	12
	[R1 = C(12), R2 = C(15)]	[R1 = C(12), R2 = C(15)]	[R1 = C(12'), R2 = C(15')]	[R1 = Si(12), R2 = Si(16)]	[R1 = C(19), R2 = C(16)]
Ti–C ₅ ^a /Å	2.027(3)	1.989(4)	1.995(4)	1.992(4)	2.054(3)
$\phi^{b/p}$	4.4	3.1	3.5	3.5	4.9
$\delta^c/\text{Å}$	0.16	0.11	0.12	0.12	0.18
Ti–N(1)/Å	2.020(2)	1.937(3)	1.930(4)	1.941(3)	2.020(2)
B–N(1)/Å	1.428(3)	1.464(6)	1.448(6)	1.436(5)	1.428(4)
B–N(2)/Å	1.409(3)	1.382(6)	1.386(6)	1.419(5)	1.414(4)
B–C(1)/Å	1.603(3)	1.602(6)	1.605(6)	1.595(5)	1.610(4)
N(1)–Ti–C ₅ ^{a/p}	99.2(1)	99.7(2)	99.7(2)	99.73(9)	99.86(10)
N(1)–B–N(2) ^o	131.0(2)	132.9(4)	131.4(4)	130.0(3)	130.6(3)
N(1)–B–C(1) ^o	103.57(18)	99.4(3)	100.1(3)	101.8(3)	104.0(2)
N(2)–B–C(1) ^o	125.5(2)	127.6(4)	128.5(4)	127.5(3)	125.4(3)
$\Sigma[X-B-Y]^{d/p}$	360.0	359.9	360.0	359.3	360.0
$\Delta B^e/\text{Å}$	0.006	0.016	0.021	0.064	0.004
B–N(2)–R1 ^o	123.2(2)	122.8(4)	123.1(4)	122.7(2)	122.1(2)
B–N(2)–R2 ^o	122.0(2)	121.8(3)	121.6(4)	115.5(2)	123.5(2)
R1–N(2)–R2 ^o	114.8(2)	115.3(3)	115.2(3)	121.6(2)	114.4(2)
$\Sigma[X-N(2)-Y]^{d/p}$	360.0	359.9	359.9	359.8	360.0
$\Delta N(2)^e/\text{Å}$	0.009	0.001	0.020	0.043	0.012
$\tau[B-N(2)]^{f/p}$	2.1	1.7	1.9	38.0	1.3
Ti–N(1)–B ^o	102.4(2)	105.8(3)	105.8(3)	102.5(2)	102.2(2)
Ti–N(1)–Ph ^o	124.2(2)	119.5(2)	119.3(2)	127.7(2)	124.7(2)
B–N(1)–Ph ^o	131.7(2)	133.4(3)	133.6(3)	129.8(3)	131.8(2)
$\Sigma[X-N(1)-Y]^{d/p}$	358.3	358.7	358.7	360.0	358.7
$\Delta N(1)^e/\text{Å}$	0.115	0.102	0.103	0.015	0.103
$\tau[N(2)-Ph]^{f/p}$	78.2	72.0	73.8	41.2	77.2
B–C(1)···[C ₅] ^{g/p}	148.6	148.2	148.9	145.3	148.2
$\Delta B[C_5]^h/\text{Å}$	0.848	0.853	0.860	0.919	0.878

^a “C₅” refers to the centroid of the five-membered aromatic ring. ^b ϕ Is the angle between the normal to the [C₅] ring plane and the Ti···C₅ ring centroid vector. ^c δ Is the offset of the Ti centre away from a position perpendicularly beneath the C₅ ring centroid. ^d Sum of the angles around the central atom. ^e ΔX is the deviation of atom X from the plane of its substituents. ^f Torsion angle about linkage. ^g Angle of B–C(1) bond to [C₅] ring plane. ^h Deviation of B from [C₅] plane.

ment (cyclopentadienyl vs. indenyl) or the boron bridge [BNiPr₂ vs. BN(SiMe₃)₂], in order to tune the electronic and steric characteristics of the complexes. Increasing the steric demand of the amido fragment in the chelating ligand by substituting phenyl for cyclohexyl or *tert*-butyl was not feasible, as the reaction of the respective ligand precursors with [Ti(NMe₂)₄] resulted only in the formation of non-bridged species. In preliminary experiments, the reported dichloro complexes could be activated with MAO for the polymerisation of ethylene and styrene. Further experiments to establish the influence of variations in the described ligand framework on the polymerisation characteristics are in progress.

Experimental

General considerations

All manipulations were carried out under a dry nitrogen atmosphere using common Schlenk techniques. Solvents were dried by standard procedures, distilled, and stored under nitrogen over molecular sieves. [Ti(NMe₂)₄] and Me₃SiCl were used as supplied without further purification. Ligand precursors were synthesised as previously reported.^{5b-d}

NMR experiments were performed on either a Varian Unity 500 spectrometer, a Bruker DPX-400 spectrometer, a JEOL-EX270 Delta Upgrade spectrometer or a Bruker Mercury 200 spectrometer. Chemical shifts for ¹H and ¹³C-¹H NMR spectra were referenced to internal solvent resonances and are reported relative to tetramethylsilane. Chemical shifts for ¹¹B-¹H and ²⁹Si-¹H NMR spectra were referenced to BF₃·OEt₂ and tetramethylsilane, respectively, as external standards. Routine coupling constants for ¹H NMR spectra are not reported. Mass spectra were recorded either on a Finnigan MAT 95, a Thermo Finnigan Trio 1000, or a Micromass Platform II spectrometer. IR spectroscopy was conducted on CH₂Cl₂ solutions and performed on a Bruker Vector 22 FT-IR

spectrometer. Elemental analyses were recorded on a Carlo-Erba elemental analyzer, model 1106.

Preparations

[Ti{ η^5 - η^1 -(C₅H₄)B(NiPr₂)NPh}(NMe₂)₂] (3). (C₅H₅)B(NiPr₂)-N(H)Ph (0.83 g, 3.09 mmol) was dissolved in 15 mL toluene and [Ti(NMe₂)₄] (0.69 g, 3.09 mmol) in 5 mL hexane was added dropwise at –78 °C. The yellow solution was stirred for 20 min at –78 °C, before warming it slowly to ambient temperature. At –10 °C, the colour changed from yellow to orange and formation of HNMe₂ was observed. After 30 min at ambient temperature, the mixture was heated to 35 °C for 15 min. The solvent was removed *in vacuo*, the red residue dissolved in 30 mL hexane and stored at –30 °C to yield pure **3** as orange crystals (1.00 g, 2.49 mmol, 80%).

Analytical data for **3** have been previously reported.⁸

[Ti{ η^5 - η^1 -(C₅H₄)B(N(SiMe₃)₂)NPh}(NMe₂)₂] (4). The same procedure was employed as for **3**. After removing all volatile components, **4** was obtained as a dark red oil (2.10 g, 4.55 mmol, 99%).

¹H NMR (CDCl₃): δ 0.11 (s, 18H, SiMe₃), 3.09 (s, 12H, NMe₂), 5.97 (m, 2H, CH_{Cp}), 6.46 (m, 2H, CH_{Cp}), 6.8–7.3 (m, 5H, CH_{Ph}). ¹³C NMR (toluene-d₈): δ 3.93 (SiMe₃), 47.44 (NMe₂), 115.56, 120.05 (CH_{Cp}), 121.65, 124.03, 128.71 (CH_{Ph}), 153.24 (*ipso*-C_{Ph}). ¹¹B NMR (toluene-d₈): δ 33.0. ²⁹Si NMR (toluene-d₈): δ 0.27. MS (CI); *m/z* (%): 329 (8) [M⁺ – Ti(NMe₂)₂ + 3H] and ligand fragments (Found: C, 54.20; H, 8.31; N, 12.01. C₂₁H₃₉BN₄Si₂Ti requires: C, 54.54; H, 8.50; N 12.12%).

[Ti{ η^5 - η^1 -(C₅H₄)B(NiPr₂)NPh}Cl₂] (5). A solution of **3** (0.17 g, 0.42 mmol) in 10 mL hexane was reacted with Me₃SiCl (0.50 g, 4.60 mmol) at 0 °C. The mixture was allowed to come to ambient temperature and stirred for 16 h. The yellow–orange precipitate was filtered off, washed with 10 mL hexane and

dried *in vacuo*. Recrystallisation from CH₂Cl₂ at 4 °C yields **5** (0.16 g, 0.42 mmol, 98%) as orange crystals.

Analytical data for **5** have been previously reported.⁸

[Ti{η⁵-C₅H₄}B(N(SiMe₃)₂)NPh]Cl₂ (6**).** The same procedure was employed as for **5**. Recrystallisation from hexane at ambient temperature yields pure **6** as orange prismatic and needle shaped crystals (0.78 g, 1.75 mmol, 68%).

¹H NMR (benzene-d₆): δ 0.10 (s, 9H, SiMe₃), 0.20 (s, 9H, SiMe₃), 5.96 (m, 1H, CH_{CP}), 6.07 (m, 1H, CH_{CP}), 6.31 (m, 1H, CH_{CP}), 6.61 (m, 1H, CH_{CP}), 6.75–7.45 (m, 5H, CH_{Ph}). ¹³C NMR (benzene-d₆): δ 3.74, 3.87 (SiMe₃), 119.01, 121.23, 122.72, 123.08, 123.25, 126.23, 126.45 (CH_{CP/Ph}), 152.65 (*ipso*-C_{Ph}). ¹¹B NMR (benzene-d₆): δ 33.1. ²⁹Si NMR (benzene-d₆): δ 1.7, 5.6 (s, SiMe₃). MS (CI); *m/z* (%): 445 (54) [M⁺], 329 (29) [M⁺ – TiCl₂ + 3H], 236 (20) [(Me₃Si)₂NBCpH⁺], 162 (60) [(Me₃Si)₂NH₂⁺] (Found: C, 45.44; H, 5.98; N, 6.30. C₁₇H₂₇BCl₂N₂Si₂Ti requires: C, 45.86; H, 6.11; N 6.29%).

[Ti{η⁵-C₅H₄}B(NiPr₂)N(H)Cy}(NMe₂)₃ (9**).** (C₅H₅)B(NiPr₂)N(H)Cy (0.75 g, 2.73 mmol) dissolved in 20 mL of toluene was treated at 0 °C with [Ti(NMe₂)₄] (0.61 g, 2.73 mmol). The reaction mixture was refluxed for 3 h while the colour changed from yellow to dark red. The solvent was removed *in vacuo* to give **9** as a dark red oil (1.23 g, 2.70 mmol, 99%) that is virtually free from impurities.

¹H NMR (toluene-d₈): δ 1.19 (d, 12H, Me_{Pr}), 0.90–2.00 (m, 10H, CH₂), 3.18 (s, 18H, NMe₂), 3.55–3.75 (m, 2H, CH_{Pr}), 5.93 (m, 2H, CH_{CP}), 6.36 (m, 2H, CH_{CP}). ¹³C NMR (toluene-d₈): δ 23.74 (Me_{Pr}), 25.75, 26.28, 38.70 (CH₂), 46.45 (CH_{Cy}), 50.30 (NMe₂), 51.20 (CH_{Pr}), 111.27, 119.71 (CH_{CP}). ¹¹B NMR (toluene-d₈): δ 28.3. MS (CI); *m/z* (%): 454 (5) [M⁺ + H], 409 (71) [M⁺ – HNMe₂], 275 (20) [M⁺ – Ti(NMe₂)₃ + 3H]. IR/cm⁻¹ 3441 w ν(NH) (Found: C, 60.32; H, 10.27; N, 15.23. C₂₃H₄₈BN₅Ti requires: C, 60.93; H, 10.67; N 15.45%).

[Ti{η⁵-C₅H₄}B(NiPr₂)N(H)*t*Bu}(NMe₂)₃ (10**).** The same procedure was employed as for **9**. Recrystallisation from hexane at –30 °C gave pure **10** as an orange microcrystalline material (1.08 g, 2.87 mmol, 99%).

¹H NMR (benzene-d₆): δ 1.16 (d, 12H, Me_{Pr}), 1.19 (s, 9H, Me_{tBu}), 3.18 (s, 18H, NMe₂), 3.51 (m, 2H, CH_{Pr}), 5.91 (m, 2H, CH_{CP}), 6.46 (m, 2H, CH_{CP}). ¹³C NMR (benzene-d₆): δ 24.00 (Me_{tBu}), 34.05 (Me_{Pr}), 46.4 (br, CH_{Pr}), 49.66 (*ipso*-C_{tBu}), 50.45 (NMe₂), 110.98, 120.87 (CH_{CP}). ¹¹B NMR (benzene-d₆): δ 29.1. MS (CI); *m/z* (%): 383 (100) [M⁺ – NMe₂], 339 (80) [M⁺ – 2NMe₂], 183 (47) [M⁺ – Ti(NMe₂)₃ – C₅H₄]. IR/cm⁻¹ 3456 w ν(NH) (Found: C, 58.75; H, 10.57; N, 16.19. C₂₁H₄₆BN₃Ti requires: C, 59.02; H, 10.85; N 16.39%).

[Ti{η⁵-C₉H₆}B(NiPr₂)NPh}(NMe₂)₂ (12**).** The same procedure was employed as for **3**. Recrystallisation twice from hexane at –30 °C and subsequently 4 °C afforded **12** (1.25 g, 2.77 mmol, 55%) as orange crystals.

¹H NMR (benzene-d₆): δ 0.91, 1.03 (br d, 3H, Me_{Pr}), 1.64 (br d, 6H, Me_{Pr}), 2.29 (s, 6H, NMe₂), 3.08 (s, 6H, NMe₂), 3.28 (m, 1H, CH_{Pr}), 3.73 (m, 1H, CH_{Pr}), 6.2–7.8 (m, 11H, CH_{Ind/Ph}). ¹³C NMR (benzene-d₆): δ 22.81, 22.03, 26.98, 27.67 (Me_{Pr}), 44.53 (CH_{Pr}), 46.40 (NMe₂), 46.99 (CH_{Pr}), 49.48 (NMe₂), 107.38, 120.44, 121.41, 123.23, 123.41, 123.61, 124.35, 124.97, 126.81 (CH_{Ind/Ph}), 128.78, 132.00 (quaternary C_{Ind}), 155.37 (*ipso*-C_{Ph}). ¹¹B NMR (benzene-d₆): δ 27.7. MS (CI); *m/z* (%): 319 (40) [M⁺ – Ti(NMe₂)₂ + 3H] (Found: C, 65.89; H, 8.03; N, 12.22. C₂₅H₃₇BN₄Ti requires: C, 66.39; H, 8.25; N 12.39%).

[Ti{η⁵-C₉H₆}B(NiPr₂)NPh]Cl₂ (13**).** The same procedure was employed as for **5**. Recrystallisation from toluene at –30 °C yields pure **13** as red microcrystals (0.17 g, 0.39 mmol, 87%).

¹H NMR (benzene-d₆): δ 0.74 (d, 3H, Me), 0.79 (d, 3H, Me), 1.44 (br d, 6H, Me), 3.13 (m, 1H, CH_{Pr}), 3.39 (m, 1H, CH_{Pr}),

6.3–7.7 (m, 11H, CH_{Ind/Ph}). ¹³C NMR (CDCl₃): δ 21.35, 21.66, 27.20, 27.71 (Me), 44.61, 47.03 (CH_{Pr}), 116.38, 121.78, 125.14, 126.16, 127.53, 127.95, 128.54, 129.18, 129.39 (CH_{Ind/Ph}), 133.45, 134.80 (quaternary C_{Ind}), 151.82 (*ipso*-C_{Ph}). ¹¹B NMR (benzene-d₆): δ 28.0. MS (EI); *m/z* (%): 314 (100) [M⁺ – TiCl₂ – 2H] (Found: C, 58.05; H, 5.65; N, 6.18. C₂₁H₂₅BCl₂N₂Ti requires: C, 57.98; H, 5.79; N 6.44%).

X-Ray crystallography

Crystal data for 5. C₁₇H₂₃BCl₂N₂Ti, *M* = 385.0, monoclinic, *P*2₁/*c* (no. 14), *a* = 12.575(2), *b* = 18.852(2), *c* = 16.8556(13) Å, β = 109.247(11)°, *V* = 3772.5(8) Å³, *Z* = 8 (two independent molecules), *D*_c = 1.356 g cm⁻³, μ(Mo-Kα) = 0.74 mm⁻¹, *T* = 183 K, orange platy needles; 6624 independent measured reflections, *F*² refinement, *R*₁ = 0.050, *wR*₂ = 0.097, 3940 independent observed reflections [|*F*_o| > 4σ(*F*_o)], 2θ_{max} = 50°, 391 parameters.

Crystal data for 6. C₁₇H₂₇BCl₂N₂Si₂Ti, *M* = 445.2, monoclinic, *P*2₁/*c* (no. 14), *a* = 7.1231(11), *b* = 19.0371(10), *c* = 17.219(2) Å, β = 97.423(14)°, *V* = 2315.4(5) Å³, *Z* = 4, *D*_c = 1.277 g cm⁻³, μ(Cu-Kα) = 6.26 mm⁻¹, *T* = 203 K, orange blocky needles; 3423 independent measured reflections, *F*² refinement, *R*₁ = 0.049, *wR*₂ = 0.126, 2855 independent observed absorption corrected reflections [|*F*_o| > 4σ(*F*_o)], 2θ_{max} = 120°, 215 parameters.

Crystal data for 12. C₂₅H₃₇BN₄Ti, *M* = 452.3, triclinic, *P*1̄ (no. 2), *a* = 9.6645(10), *b* = 9.8449(13), *c* = 13.8532(14) Å, α = 88.386(10), β = 80.406(8), γ = 75.145(9)°, *V* = 1256.1(2) Å³, *Z* = 2, *D*_c = 1.196 g cm⁻³, μ(Mo-Kα) = 0.36 mm⁻¹, *T* = 203 K, orange blocks; 4427 independent measured reflections, *F*² refinement, *R*₁ = 0.052, *wR*₂ = 0.132, 3445 independent observed reflections [|*F*_o| > 4σ(*F*_o)], 2θ_{max} = 50°, 272 parameters.

CCDC reference numbers 225922 (**5**), 225923 (**6**) and 225924 (**12**).

See <http://www.rsc.org/suppdata/dt/b3/b315708c/> for crystallographic data in CIF or other electronic format.

Acknowledgements

This work was supported by BASF AG Ludwigshafen, BMBF, DFG, EPSRC, R. Soc. F. M. B. thanks the Fonds der Chemischen Industrie for a doctoral scholarship.

References

- (a) H. H. Brintzinger, D. Fischer, R. Mülhaupt, B. Rieger and R. M. Waymouth, *Angew. Chem., Int. Ed. Engl.*, 1995, **34**, 1143, and references therein; (b) W. Kaminsky, *J. Chem. Soc., Dalton Trans.*, 1998, 1413, and references therein.
- P. J. Shapiro, E. Bunel, W. Schaefer and J. E. Bercaw, *Organometallics*, 1990, **9**, 867.
- (a) A. L. McKnight and R. M. Waymouth, *Chem. Rev.*, 1998, **98**, 2587, and references therein; (b) G. J. P. Britovsek, V. C. Gibson and D. F. Wass, *Angew. Chem., Int. Ed. Engl.*, 1999, **38**, 428, and references therein; (c) V. C. Gibson and S. K. Spitzmesser, *Chem. Rev.*, 2003, **103**, 283, and references therein.
- S. Chum, W. J. Kruper and M. J. Guest, *Adv. Mater.*, 2000, **12**, 1759.
- (a) H. Braunschweig, C. v. Koblinki, M. Neugebauer, U. Englert and X. Zheng, *J. Organomet. Chem.*, 2001, **619**, 305; (b) H. Braunschweig, C. v. Koblinki, F. M. Breitling, K. Radacki, C. Hu, L. Wesemann, T. Marx and I. Pantenburg, *Inorg. Chim. Acta*, 2003, **350**, 467; (c) H. Braunschweig, M. Kraft, M. Homberger, F. M. Breitling, A. J. P. White, U. Englert and D. J. Williams, *Appl. Organomet. Chem.*, 2003, **17**, 421; (d) H. Braunschweig, F. M. Breitling, M. Homberger, C. v. Koblinki, A. J. P. White and D. J. Williams, *Z. Anorg. Allg. Chem.*, 2003, **629**, 2244.
- (a) H. Braunschweig, C. v. Koblinki and M. O. Kristen, *Ger. Pat. Appl.*, DE 19858016A1, 1998; (b) H. Braunschweig, C. v. Koblinki and R. Wang, *Eur. J. Inorg. Chem.*, 1999, 69; (c) H. Braunschweig,

- C. v. Koblinski, M. Mamuti, U. Englert and R. Wang, *Eur. J. Inorg. Chem.*, 1999, 1899.
- 7 A. J. Ashe, III, X. Fang and J. W. Kampf, *Organometallics*, 1999, **18**, 2288.
- 8 H. Braunschweig, C. v. Koblinski and U. Englert, *Chem. Commun.*, 2000, 1049.
- 9 For reviews on boron-bridged Group IV metallocenes and related compounds, see: (a) P. J. Shapiro, *Eur. J. Inorg. Chem.*, 2001, 321; (b) H. Braunschweig, F. M. Breitling, E. Gullo and M. Kraft, *J. Organomet. Chem.*, 2003, **680**, 31; (c) S. Aldridge and C. Bresner, *Coord. Chem. Rev.*, 2003, **244**, 71.
- 10 J. A. Klang and D. B. Collum, *Organometallics*, 1988, **7**, 1532.
- 11 C. v. Koblinski, PhD Thesis, RWTH Aachen, 2000.
- 12 B. Wrackmeyer, *Prog. NMR Spectrosc.*, 1979, **12**, 227.
- 13 H. Braunschweig and F. M. Breitling, unpublished results.